

## Waterlike anomalies for core-softened models of fluids: One dimension

M. Reza Sadr-Lahijany, Antonio Scala, Sergey V. Buldyrev, and H. Eugene Stanley

Center for Polymer Studies and Department of Physics, Boston University, Boston, Massachusetts 02215

(Received 23 July 1999)

We use a one-dimensional (1D) core-softened potential to develop a physical picture for some of the anomalies present in liquid water. The core-softened potential mimics the effect of hydrogen bonding. The interest in the 1D system stems from the facts that closed-form results are possible and that the qualitative behavior in 1D is reproduced in the liquid phase for higher dimensions. We discuss the relation between the shape of the potential and the density anomaly, and we study the entropy anomaly resulting from the density anomaly. We find that certain forms of the two-step square-well potential lead to the existence at  $T=0$  of a low-density phase favored at low pressures and of a high-density phase favored at high pressures, and to the appearance of a point  $C'$  at a positive pressure, which is the analog of the  $T=0$  “critical point” in the 1D Ising model. The existence of point  $C'$  leads to anomalous behavior of the isothermal compressibility  $K_T$  and the isobaric specific heat  $C_p$ . [S1063-651X(99)06012-2]

PACS number(s): 61.20.Gy, 61.25.Em, 65.70.+y, 64.70.Ja

### I. INTRODUCTION

Water, the most common liquid on earth, is uncommon in many of its properties. For example, water at ambient pressure has an anomalous density behavior, as for  $T < 4$  °C its density decreases upon cooling. The subject of liquid anomalies is not limited to the density anomaly. Two other anomalies are the increase of isothermal compressibility  $K_T$  (density fluctuations) and of the isobaric specific heat  $C_p$  (entropy fluctuations) upon cooling. All these anomalies occur in liquid water [1] and some occur also in other liquids [1–3].

In their pioneering work, Stell and Hemmer investigated potentials that have a region of negative curvature in their repulsive core [4] (henceforth referred to as core-softened potentials) in relation to the possibility of a new critical point in addition to the normal liquid-gas critical point. They also pointed out that for the one-dimensional (1D) model with a long-range attractive tail, the isobaric thermal expansion coefficient,  $\alpha_p \equiv V^{-1}(\partial V/\partial T)_p$  (where  $V$ ,  $T$ , and  $P$  are the volume, temperature, and pressure), can take an anomalous negative value. Debenedetti *et al.*, using general thermodynamic arguments, confirmed that a “softened core” can lead to  $\alpha_p < 0$  [5]. Stillinger and collaborators found  $\alpha_p < 0$  for a 3D system of particles interacting by purely repulsive interactions—a Gaussian potential [6].

In this work, we investigate the relation of a core-softened potential to the liquid anomalies mentioned above. *Ab initio* calculations [7] and inversion of structure factor data [7,8] revealed that a core-softened potential can be considered a realistic first-order approximation for the interaction of many materials with anomalous behavior [8,9], even in the case of network forming anomalous liquids [1]. A recent work has showed that the anomalous behavior of a 1D model can be reproduced in two dimensions (2D) as well [10,11].

Here we will provide the details necessary to understand the preliminary results announced in [10]. Specifically, we investigate thoroughly an exactly solvable 1D model in order to develop an intuitive picture of how the core-softened potential can lead to all three anomalies and to relate the oc-

currence of these anomalies to the shape and parameters of the potential. We also discuss the possible existence of a second critical point and its relation to the parameters of the model.

The core-softened potential that we study is (Fig. 1)

$$u(r) = \begin{cases} \infty, & 0 < r < a \\ -\lambda\epsilon, & a < r < b \\ -\epsilon, & b < r < c \\ 0, & r > c, \end{cases} \quad (1)$$

where  $r$  is the particle separation. The potential is composed of a “hard core” of diameter  $a$  which has a repulsive shoulder (henceforth referred to as “softened core”) of width  $(b - a)$  and depth  $\lambda\epsilon$ , and an attractive well of width  $(c - b)$  and depth  $\epsilon$ . Unless specified otherwise, our numerical calculations are for the choice of values  $a=1$ ,  $b=1.4$ ,  $c=1.7$ ,  $\epsilon=2$ , and  $\lambda=0.5$  [12]. A similar potential was introduced by Ben-Naim to model water anomalies [13,14]. A continuous potential of an analogous form models the interaction between clusters of strongly bonded pentamers of water [15].

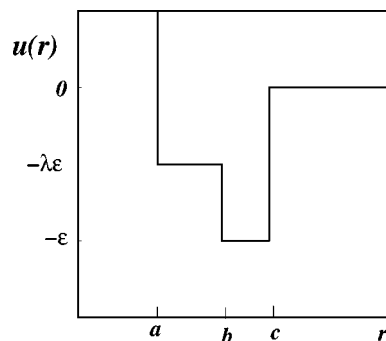


FIG. 1. General form for the core-softened potential  $u(r)$  studied here. The length parameters  $a, b, c$  and energy parameters  $\epsilon, \lambda$  are shown (both sets in arbitrary units).

This type of interaction qualitatively reproduces the density anomaly of water. At sufficiently low pressures and temperatures, nearest-neighbor pairs are separated by a distance  $r \approx b$  to minimize the energy. As temperature increases, the system explores a larger portion of the configurational space in order to gain more entropy. This includes the penetration of particles into the softened core, which can cause an anomalous contraction upon heating.

The relation between the density anomaly and the shape of the potential can also be understood using the thermodynamic relation

$$(\partial V / \partial T)_P = \beta^2 (P \langle (\delta V)^2 \rangle_{PT} + \langle \delta V \delta E \rangle_{PT}), \quad (2)$$

where  $\beta \equiv 1/k_B T$  with  $k_B$  being the Boltzmann factor,  $E$  is the energy, and  $\langle \dots \rangle_{PT}$  is the thermodynamic average in a constant  $P$ , constant  $T$  ensemble. For a system with a density anomaly, the left-hand side of Eq. (2) is negative at temperatures below the temperature of maximum density  $T_{MD}$ . The first term on the right-hand side, proportional to the square of the volume fluctuations, is always positive. Thus below  $T_{MD}$  the second term must be negative, which requires anticorrelation between the fluctuations in  $E$  and  $V$ . This kind of anticorrelation exists for the core-softened model when the fluctuations occur between the states with  $r \approx b$  and the states with  $r \approx a$ , which have a larger energy but a smaller volume. We conclude that the core-softened potential is a candidate for generating the density anomaly.

The paper is organized as follows. In Sec. II we present the exact solution for the Gibbs potential. Sections III–VI discuss the anomalies in the density and entropy, and their response functions compressibility and specific heat. In Sec. VII we discuss interesting analogies with the Ising model. Finally, Sec. VIII interprets the anomalies in terms of two different local structures.

## II. EXACT SOLUTION FOR GIBBS POTENTIAL

To derive the Gibbs potential for the model, we choose  $c < 2a$  to restrict the interactions to nearest neighbors. The 1D model is then exactly solvable using standard methods [13,14,16]. The partition function is (see Appendix A)

$$Z(T, P) = \frac{1}{(\Delta V) [\Lambda(T)]^N (\beta P)^2} [\Omega(T, P)]^{N-1}, \quad (3)$$

where  $N$  is the number of particles,  $\Delta V$  is a discretization factor which is needed for keeping  $Z$  dimensionless and does not enter the equation of state, and  $\Lambda(T)$  is the De Broglie wavelength. Here

$$\Omega(T, P) \equiv \int_0^\infty dx e^{-\beta P x} e^{-\beta u(x)}, \quad (4)$$

where  $u(x)$  is the interaction potential.

The Gibbs potential  $G(T, P) \equiv -k_B T \ln Z(T, P)$  is then

$$G(T, P) = -k_B T [(N-1) \ln \Omega(T, P) - N \ln \Lambda(T) - 2 \ln P - \ln \Delta V]. \quad (5)$$

In the thermodynamic limit  $N \rightarrow \infty$ , the terms  $2 \ln P$  and  $\ln \Delta V$  are negligible compared to the other extensive (order  $N$ ) terms.

Equation (3) is valid for any 1D system in which each particle interacts only with its nearest neighbors. If the interaction potential is given by Eq. (1), then

$$\Omega(T, P) = \frac{1}{\beta P} \Psi(T, P), \quad (6)$$

where (see Appendix A)

$$\Psi(T, P) \equiv [\phi^\lambda \theta_a + (\phi - \phi^\lambda) \theta_b + (1 - \phi) \theta_c] \quad (7)$$

and  $\theta_x(P, T) \equiv e^{-\beta P x}$ ,  $\phi(T) \equiv e^{\beta \epsilon}$ .

## III. DENSITY ANOMALY

We calculate the equation of state using the definition  $V \equiv \partial G(T, P) / \partial P$ . From Eq. (5) we find that, in the thermodynamic limit  $N \rightarrow \infty$ , the average ‘‘volume’’ (length in 1D) per particle is

$$v \equiv V/N = -\frac{k_B T}{\Omega(T, P)} \frac{\partial \Omega(T, P)}{\partial P}. \quad (8)$$

Using Eqs. (6) and (8), we find the equation of state

$$v = \frac{k_B T}{P} - \frac{k_B T}{\Psi(T, P)} \frac{\partial \Psi(T, P)}{\partial P}, \quad (9)$$

where

$$\frac{\partial \Psi(T, P)}{\partial P} = -\beta [(\phi^\lambda a \theta_a + (\phi - \phi^\lambda) b \theta_b + (1 - \phi) c \theta_c)]. \quad (10)$$

In the high-temperature limit where  $\phi \rightarrow 1$  and  $\theta_x \rightarrow 1$ , the equation of state (9) tends to

$$v = \frac{k_B T}{P} + a \quad (T \rightarrow \infty), \quad (11)$$

the equation of state for an ‘‘ideal gas’’ of rods, that is, a system of noninteracting rods of length  $a$ .

At  $T=0$ ,  $v$  as a function of  $P$  has a discontinuity at

$$P = P_{\text{up}} \equiv \frac{(1-\lambda)\epsilon}{b-a}, \quad (12)$$

which we call the upper transition pressure. At  $T=0$ ,

$$v = \begin{cases} b, & P < P_{\text{up}} \\ a, & P > P_{\text{up}}. \end{cases} \quad (13)$$

We will return to this first-order transition in Sec. VIII.

Next we study the equation of state for fixed pressure. For each value of  $P$ , we find the value of  $v(T)$  using Eq. (9) (Fig. 2). These isobars separate into two different groups.

(i) For  $P > P_{\text{up}}$ ,  $v$  increases monotonically with  $T$ , starting from its minimal value  $v=a$ . At these high pressures, the nearest neighbors are pushed inside the softened core and, as a result, the density anomaly does not occur.

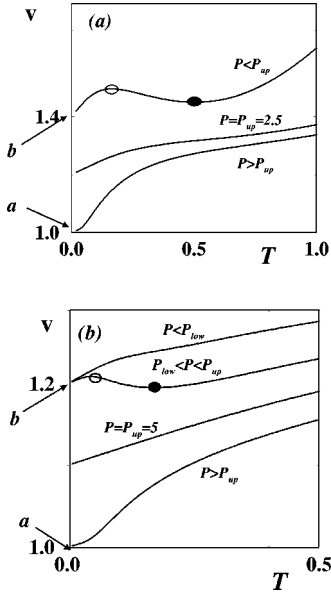


FIG. 2. Isobars of  $v$ , the average length per particle, for the discrete 1D core-softened potential showing the conditions under which a  $T_{MD}$  and  $T_{mD}$  exist. (a) The parameter values are  $a=1$ ,  $b=1.4$ ,  $c=1.7$ ,  $\epsilon=2$ , and  $\lambda=0.5$ . These values along with setting  $k_B$  and the mass of the particles to unity determine the units. From Eq. (12), these values result in  $P_{up}=2.5$ .  $P_{low}$  is almost zero, so no  $P < P_{low}$  isobar is shown. The  $T_{MD}$  point is marked by a filled ellipse and the  $T_{mD}$  point by an open ellipse. (b) The parameter values are  $a=1$ ,  $b=1.2$ ,  $c=1.7$ ,  $\epsilon=2$ ,  $\lambda=0.5$  and thus from Eq. (12),  $P_{up}=5$ . Now  $P_{low} \approx 3.3$ , so a  $P < P_{low}$  isobar is shown.

(ii) When  $P$  is lowered just below  $P_{up}$ ,  $v=b$  at  $T=0$  [Eq. (13)], and the  $v(T)$  isobars show a maximum at a temperature of minimum density  $T_{mD}$  and a minimum at  $T_{MD}$  [3,6,13,14,17]. For  $P < P_{up}$ , the system starts at  $T=0$  from the bottom of the energy well at  $v=b$ . Upon heating, the particles first start to explore the wider region in the bottom of the potential well and the system expands. At higher temperatures, the particles penetrate the softened core and the system shrinks, showing an anomalous temperature-driven contraction. For even higher temperatures, the particles move outside of the potential well, causing the system to expand.

The minimum density point  $T_{mD}$  is of interest. In real liquids with  $T_{MD}$ ,  $T_{mD}$  is rarely observed [3], possibly because it would be located at a low temperature, where the liquid phase is not stable. As pressure is lowered further, the maximum and minimum density points coincide at some point  $(T_{low}, P_{low})$ , which can be found from the system of equations  $(\partial v / \partial T)_P = 0$  and  $(\partial^2 v / \partial T^2)_P = 0$ . We have observed this behavior upon changing the parameters of the interaction potential [see, e.g., Fig. 2(b)]. For  $P < P_{low}$ , no density anomaly is observed, as shown in Fig. 2(b).

#### IV. ISOTHERMAL COMPRESSIBILITY ANOMALY

The isothermal compressibility is defined as

$$K_T \equiv -\frac{1}{V} \left( \frac{\partial V}{\partial P} \right)_T = \frac{1}{\rho} \left( \frac{\partial \rho}{\partial P} \right)_T. \quad (14)$$

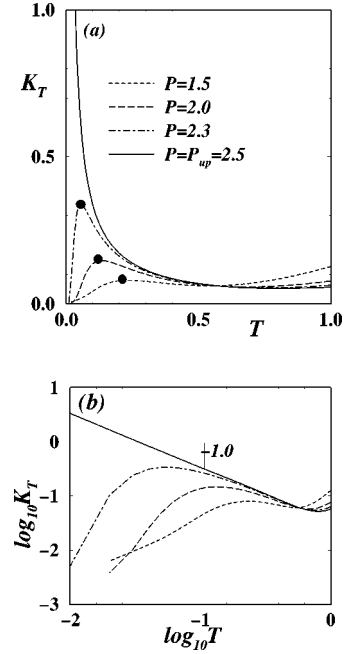


FIG. 3. Isothermal compressibility for the same parameter values and units as Fig. 2(a). (a) Isothermal compressibility along different isobars, with their maxima marked by filled circles.  $K_T$  along the isobar  $P_{up}$  diverges as  $T \rightarrow 0$ . (b) Log-log plot of the same results showing the divergence of  $K_T$  as  $1/T$  along the critical isobar  $P = P_{up}$ .

$K_T$  is thus the response of the volume to its conjugate variable pressure and it is proportional to fluctuations in specific volume,

$$K_T \propto \langle (\delta V)^2 \rangle. \quad (15)$$

For most materials  $(\partial K_T / \partial T)_P > 0$ , so fluctuations decrease upon cooling. In the case of water, for a wide range of pressures,  $K_T$  passes through a minimum and shows an anomalous increase upon cooling. Along the  $P=1$  atm isobar, for example, the minimum compressibility point is around  $46^\circ\text{C}$  [1].

From Eq. (9) and Eq. (14), we find

$$K_T = \frac{1}{\beta V} \left[ \frac{1}{P^2} + \frac{1}{\Psi(T, P)} \frac{\partial^2 \Psi(T, P)}{\partial P^2} - \left( \frac{1}{\Psi(T, P)} \frac{\partial \Psi(T, P)}{\partial P} \right)^2 \right], \quad (16)$$

where

$$\frac{\partial^2 \Psi(T, P)}{\partial P^2} = \beta^2 [\phi^\lambda a^2 \theta_a + (\phi - \phi^\lambda) b^2 \theta_b + (1 - \phi) c^2 \theta_c]. \quad (17)$$

Figure 3 shows  $K_T$  as a function of  $T$  along isobars from Eq. (16). As  $T \rightarrow \infty$ ,  $K_T$  tends to its ideal gas value  $1/P$ , which is also predicted by Eq. (11). As  $T \rightarrow 0$ , using Eq. (14), we find

$$K_T \rightarrow 0 \quad (T \rightarrow 0, P \neq P_{up}). \quad (18)$$

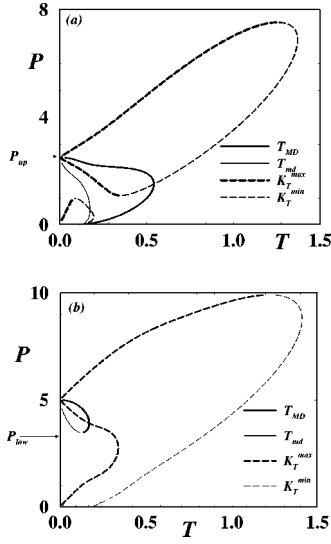


FIG. 4. The loci of the two density extrema ( $T_{MD}$  and  $T_{mD}$ ) and the two  $K_T$  extrema ( $K_T^{\max}$  and  $K_T^{\min}$ ) for the discrete potential of Fig. 1; (a) with the same parameter values and units as Fig. 2(a), so  $P_{up}=2.5$  and  $P_{low}\approx 0$ ; the locus of  $K_T$  extrema has two ‘‘loops,’’ one connected to the point  $C'(T=0, P=P_{up})$  and the second to the point  $C(T=0, P=0)$ , and (b) with the same parameter values and units as Fig. 2(b), for which  $P_{up}=5$  and  $P_{low}\approx 3.3$ ; the two ‘‘loops’’ now join.

As  $T$  decreases from infinity to zero,  $K_T$  passes through two extrema, a minimum and a maximum, between which  $(\partial K_T/\partial T)_P < 0$ . Thus the 1D core-softened model generates a compressibility anomaly.

## V. DENSITY AND COMPRESSIBILITY EXTREMA LINES

The locus of the points  $T_{MD}$  in the  $P$ - $T$  phase diagram is of special interest. For water, the shape of the  $T_{MD}$  line helps distinguish between different scenarios proposed to explain water’s anomalies [18–20]. In simulations [21–23], the  $T_{MD}$  line presents a ‘‘nose,’’ i.e., a point in which as  $P$  decreases the slope changes from negative to positive passing through an infinite value (Fig. 4).

In Fig. 4, we present the  $T_{MD}$  and  $T_{mD}$  with the same parameters as in Fig. 2. We observe that both lines originate at  $P_{up}$  [25] and terminate at  $P_{low}$ . Moreover, the  $T_{MD}$  line has a negative slope for large  $P$  which is in agreement with experimental water and for lower  $P$  the slope of the  $T_{MD}$  line changes sign and so a nose is present.

As shown in Fig. 4, the locus of extrema in compressibility intersects the  $T_{MD}$  line at its nose, as predicted by Sastry *et al.* [19] using thermodynamic relations. Moreover, whenever the  $T_{MD}$  line has a negative slope, the compressibility must increase upon cooling in the region to the left of the  $T_{MD}$  line [19], resulting in a line of  $K_T$  maxima which originates from the point  $C'(T=0, P=P_{up})$ .

Noteworthy is the existence of a starting and ending point for the  $T_{MD}$  line. The starting point is the point  $C'(T=0, P=P_{up})$ , and the ending point  $(T_{low}, P_{low})$ , where  $T_{mD}$  and  $T_{MD}$  meet. In Fig. 4(b) we show that the overall phase diagram does not change qualitatively upon varying the parameters of the potential.

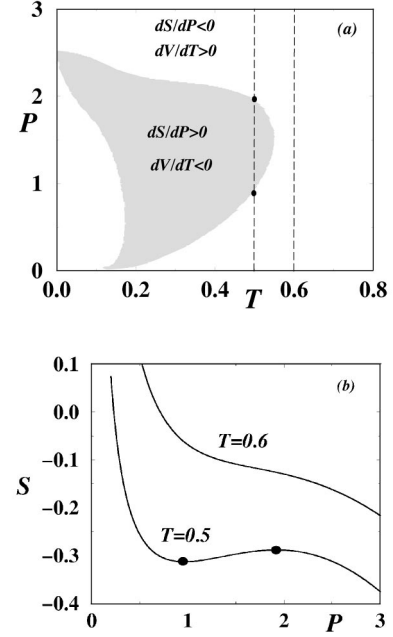


FIG. 5. (a) The region of the  $P$ - $T$  plane where the density and entropy are anomalous (gray), from Fig. 4(a). (b) The behavior of the entropy along two different isotherms. The  $T=0.5$  isotherm intersects the anomalous region and shows the maximum and minimum marked in both figures by the closed circles. The  $T=0.6$  isotherm is outside the anomalous region and does not show any anomaly.

## VI. ENTROPY ANOMALY

Since  $(\partial S/\partial P)_T = -(\partial V/\partial T)_P$ , if  $(\partial V/\partial T)_P < 0$ , then

$$\left(\frac{\partial S}{\partial P}\right)_T > 0. \quad (19)$$

Equation (19) is anomalous because, contrary to intuition, compressing the system at constant  $T$  increases its entropy [24]. To calculate the entropy from Eq. (5), we use  $S \equiv -(\partial G/\partial T)_P$ . We obtain

$$s \equiv \frac{S}{Nk_B} = \frac{3}{2} + \ln[\Psi(T, P)/(\Lambda\beta P)] - \frac{\beta}{\Psi(T, P)} \frac{\partial \Psi(T, P)}{\partial \beta}, \quad (20)$$

where

$$\begin{aligned} \frac{\partial \Psi(T, P)}{\partial \beta} &= (\epsilon\lambda - Pa)\phi^\lambda \theta_a + \epsilon(\phi - \lambda\phi^\lambda)\theta_b \\ &\quad - (\phi - \phi^\lambda)Pb\theta_b - \epsilon\phi\theta_c \\ &\quad - (1 - \phi)Pc\theta_c. \end{aligned} \quad (21)$$

Using Eq. (20), we plot the entropy for two isotherms (Fig. 5). For  $T=0.6$ , there is no density anomaly [Fig. 5(a)] and hence no entropy anomaly. For  $T=0.5$ , there is a density anomaly and hence an entropy anomaly; Fig. 5(b) shows this anomalous increase of  $S$  as a function of  $P$ .

## VII. ANALOGIES WITH THE ISING MODEL

### A. First critical point

The gas-liquid first-order transition line ending at a critical point which is present in higher dimensions shrinks to the point  $C \equiv (T=0, P=0)$  for a 1D fluid in which the particles interact with an attractive potential. This point  $C$  is the remnant of what is a critical point in higher dimensions: for example,  $K_T$  diverges for  $T \rightarrow 0$ ,

$$K_T \sim 1/T \quad (T \rightarrow 0, P=0), \quad (22)$$

analogous to the divergence of the magnetic susceptibility  $\chi_T$  along the zero field line  $H=0$  for the 1D Ising model,

$$\chi_T \sim 1/T \quad (T \rightarrow 0, H=0). \quad (23)$$

The constant-pressure specific heat  $C_P \equiv T(\partial S/\partial T)_P$  is obtained from Eq. (20), with the result

$$\frac{C_P}{Nk_B} = \frac{3}{2} + \beta^2 \left[ \frac{1}{\Psi(T,P)} \frac{\partial^2 \Psi(T,P)}{\partial \beta^2} - \left( \frac{1}{\Psi(T,P)} \frac{\partial \Psi(T,P)}{\partial \beta} \right)^2 \right]. \quad (24)$$

For small  $P$  and  $T$ , the specific heat has the form

$$C_P \sim a_0 + a_2(\beta P)^2, \quad (25)$$

the analog of the Ising case for small  $H$  and  $T$  [27],

$$C_H \sim a_0 + a_2(\beta H)^2. \quad (26)$$

These features are common to model 1D fluids with attractive potentials.

### B. Second critical point

Next we will discuss the ‘‘remnant’’ of a second critical point for our core-softened model. In addition to the divergence along the  $P=0$  isobar, we find a divergence along the  $P=P_{\text{up}}$  isobar (Fig. 3),

$$K_T \sim \frac{1}{T} \quad [T \rightarrow 0, P=P_{\text{up}}]. \quad (27)$$

We also observe from Eq. (13) and Fig. 2 that there is a discontinuity in the order parameter  $v$  when crossing  $C'$  ( $P=P_{\text{up}}, T=0$ ) along the  $T=0$  axis; this is the analog of what happens to the magnetization when crossing the  $H=0$  point along the  $T=0$  axis for the Ising model.

Next we consider  $C_P$ . Taking the limit  $T \rightarrow 0$  of Eq. (24) and defining  $H \equiv |P - P_{\text{up}}|$ , we find

$$C_P = \frac{3}{2} + \frac{wA^2}{(1+w)^2} (\beta H)^2, \quad (28)$$

where we have introduced the parameters  $A \equiv b - a$  and  $w \equiv \exp(-\beta AH)$ . Equation (28) is the analog of  $C_H$  for the Ising model. Figure 6 shows the anomalous behavior of  $C_P$  as a function of  $T$  along different isobars.

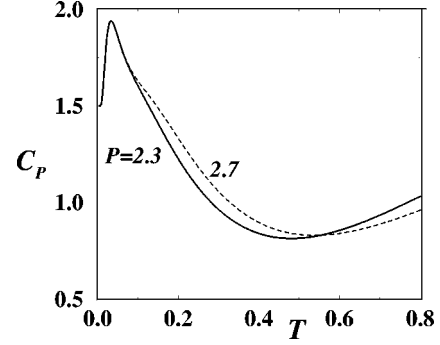


FIG. 6. Constant-pressure specific heat for the same parameter values and units as Fig. 2(a), along different isobars,  $P=2.7=P_{\text{up}}+0.2$  and  $P=2.3=P_{\text{up}}-0.2$ . Near  $T=0$ , the two curves coincide, as predicted by Eq. (28), since the values of  $H=|P-P_{\text{up}}|$  are identical.

It is interesting to note that simulations of water using the ST2 potential display a compressibility anomaly due to the presence of a second critical point in the metastable region of the liquid [22,28], and a line of  $K_T$  maxima originates from this second critical point.

## VIII. INTERPRETATION IN TERMS OF TWO LOCAL STRUCTURES

The density and compressibility anomalies can be related to the interplay between two local structures: an open structure in which the nearest-neighbor particles are typically at a distance  $b$ , and a denser structure in which the nearest neighbors penetrate into the softened core and are typically at a smaller distance  $a$ . The favored local structure is determined by the Gibbs potential per particle,

$$g(T,P) = \min_v \{u + Pv - Ts\}, \quad (29)$$

which is shown in Fig. 7 as a function of the volume per particle at  $T=0$  for two different values of  $P$ . For  $P < P_{\text{up}}$  and  $T=0$ , the minimum corresponds to the ‘‘open structure’’ with  $r \approx b$ . Increasing  $P$  increases the value of  $u + Pv - Ts$  for the open structure (Fig. 7). For  $P > P_{\text{up}}$ , the minimum corresponds to the ‘‘dense structure’’ with  $r \approx a$ .

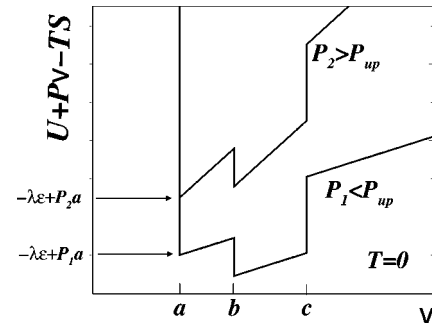


FIG. 7. Schematic plot of the function  $u + Pv - Ts$  at  $T=0$  for the core-softened potential of Fig. 1, in arbitrary units equivalent to that of Fig. 1. The equilibrium value of  $v(P)$  is determined as the absolute minimum, which is located at  $v=b$  for  $P_1 < P_{\text{up}}$  and at  $v=a$  for  $P_2 > P_{\text{up}}$ .

The value of  $P_{\text{up}}$  of Eq. (12) can also be found by equating  $u + Pv - Ts$  (at  $T=0$ ) for the two local minima, which results in

$$P_{\text{up}} = -(u_{\text{open}} - u_{\text{dense}})/(v_{\text{open}} - v_{\text{dense}}). \quad (30)$$

Substituting  $u_{\text{open}} = -\epsilon, u_{\text{dense}} = -\lambda\epsilon, v_{\text{open}} = b, v_{\text{dense}} = a$  results in the same expression as Eq. (12).

For higher dimensions, Eq. (30) helps to estimate the pressure region in which a transition between a dense and an open structure could happen. For  $d=1$ , the contribution of the  $Ts$  term makes the double-well structure of Fig. 4 disappear when  $T>0$ . This may not be true in higher dimensions. If we assume that the qualitative shape for  $d>1$  changes little from the  $d=1$  case, then for  $d>1$  there can exist a first-order transition line for small  $T$ , eventually terminating in a critical point  $C'$ .

## IX. SUMMARY

We used a 1D core-softened potential, which mimics the effect of hydrogen bonding, to develop a physical picture for some of the anomalies present in liquid water. We discussed the relation between the shape of the potential and the anomalies in density and entropy and their associated response functions  $K_T$  and  $C_p$ . The form of the potential leads to the existence at  $T=0$  of a low-density phase (favored at low pressures) and of a high-density phase (favored at high pressures), and to the appearance of a point  $C'$  at a positive pressure, which is the analog of the  $T=0$  ‘‘critical point’’ in the 1D Ising model.

## ACKNOWLEDGMENTS

We thank M. Canpolat, E. La Nave, M. Meyer, S. Sastry, F. Sciortino, A. Skibinsky, R. J. Speedy, F. W. Starr, G. S. Stell, and D. Wolf, for enlightening discussions, and NSF for support.

## APPENDIX A: DERIVATION OF THE FREE ENERGY FOR THE 1D CORE-SOFTENED MODEL

We start from the general definition of the partition function

$$\begin{aligned} Z(T, P) &\equiv \frac{1}{(\Delta V)N!h^N} \int_0^\infty dV e^{-\beta PV} \\ &\times \int d^N p d^N x e^{-\beta \mathcal{H}(p_1, \dots, p_N, x_1, \dots, x_N)}, \end{aligned} \quad (A1)$$

where  $N$  is the number of particles,  $V$  is the 1D system size,  $x_i$  and  $p_i$  are the position and momentum of particle  $i$ , respectively, and  $\mathcal{H}(p_1, \dots, p_N, x_1, \dots, x_N)$  is the Hamiltonian of the system.  $\Delta V$  is a discretization factor for  $V$ , which is needed for keeping  $Z$  dimensionless and does not enter any equation of state. The Hamiltonian can be partitioned into its kinetic and potential parts,

$$\mathcal{H}(p_1, \dots, p_N, x_1, \dots, x_N) \equiv \sum_{i=1}^N \frac{p_i^2}{2m} + U(x_1, \dots, x_N). \quad (A2)$$

One can separate Eq. (A1) into a momentum and a configurational integral, where the momentum part is

$$Z_p(T) \equiv \frac{1}{h^N} \int d^N p \exp\left(-\beta \sum_{i=1}^N \frac{p_i^2}{2m}\right). \quad (A3)$$

This integral can be written as the product of  $N$  integrals over momenta, and then using the Gaussian integral formula [29] we find

$$Z_p(T) = \frac{1}{h^N} \left( \int_{-\infty}^{\infty} dp \exp(-\beta p^2/2m) \right)^N = [\Lambda(T)]^{-N}, \quad (A4)$$

where  $\Lambda(T)$ , which has the dimension of length, is the temperature-dependent De Broglie wavelength  $\Lambda(T) \equiv h/\sqrt{2\pi mk_B T}$ . Thus the partition function takes the form

$$\begin{aligned} Z(T, P) &= \frac{1}{(\Delta V)N!\Lambda(T)^N} \\ &\times \int_0^\infty dV e^{-\beta PV} \int d^N x e^{-\beta U(x_1, \dots, x_N)}. \end{aligned} \quad (A5)$$

In order to take further steps, we use the fact that the range of interaction is less than twice the hard core ( $c < 2a$ ). As a result, one can think of the particles in the 1D system as a chain, in which each particle interacts only with its two nearest neighbors. Thus for each arrangement of the particles, we can write the interaction potential  $U$  as the sum of  $N-1$  terms,

$$\begin{aligned} U(x_1, \dots, x_N) &= U(x_N - x_{N-1}) + U(x_{N-1} - x_{N-2}) + \dots \\ &+ U(x_2 - x_1). \end{aligned} \quad (A6)$$

Using Eq. (A6), we rewrite Eq. (A5) as

$$\begin{aligned} Z(T, P) &= \frac{1}{(\Delta V)\Lambda(T)^N} \int_0^\infty dV e^{-\beta PV} \int_0^V dx_N \int_0^{x_N} dx_{N-1} \\ &\times E(x_N - x_{N-1}) \times \int_0^{x_{N-1}} dx_{N-2} \\ &\times E(x_{N-1} - x_{N-2}) \dots \int_0^{x_2} dx_1 E(x_2 - x_1), \end{aligned} \quad (A7)$$

where  $E$  is defined as

$$E(x) \equiv e^{-\beta U(x)}. \quad (A8)$$

In Eq. (A7) we have used the symmetry of  $Z$  under permutation of the particles and thus have written Eq. (A7) only for a specific order of particles, in which  $x_1 < x_2 < \dots < x_N$ . All other permutations are equivalent to this integral, after re-

numbering the particles. This results in a permutation factor  $N!$  which has canceled the  $N!$  factor in the denominator. We rewrite Eq. (A7) as

$$Z(T, P) = \frac{1}{(\Delta V)\Lambda(T)^N} \int_0^\infty dV e^{-\beta P V} F_N(V), \quad (\text{A9})$$

where we have introduced the function  $F_i(x)$ , defined recursively as

$$F_N(V) \equiv \int_0^V dx_N F_{N-1}(x_N) = (1 * F_{N-1})(V), \quad (\text{A10})$$

$$\begin{aligned} F_i(x_{i+1}) &\equiv \int_0^{x_{i+1}} dx_i E(x_{i+1} - x_i) F_{i-1}(x_i) \\ &= (E * F_{i-1})(x_{i+1}), \end{aligned} \quad (\text{A11})$$

$$F_0(x_1) \equiv 1. \quad (\text{A12})$$

The star operator  $*$  represents the binary convolution functional defined as

$$(f * g)(x) \equiv \int_0^x dy f(x-y) g(y). \quad (\text{A13})$$

We further use the notation  $\mathcal{L}[f]$  for the Laplace transformation functional, which is defined as

$$\mathcal{L}[f](z) \equiv \int_0^\infty e^{-zx} f(x), \quad (\text{A14})$$

to find the following simple form for the partition function:

$$Z(T, P) = \frac{1}{(\Delta V)\Lambda(T)^N} \mathcal{L}[F_N](\beta P). \quad (\text{A15})$$

Note that according to Eqs. (A10), (A12), and (A15),

$$Z(T, P) = \frac{1}{(\Delta V)\Lambda(T)^N} \mathcal{L}[1 * \overbrace{(E * (E * \dots (E * 1) \dots))}^{N-1}](\beta P). \quad (\text{A16})$$

Next we use the convolution theorem, which states that the Laplace transform of the convolution is equal to the product of the Laplace transforms of each function [29],

$$\mathcal{L}[f * g](z) = \mathcal{L}[f](z) \times \mathcal{L}[g](z), \quad (\text{A17})$$

and also the formula for the Laplace transform of a constant function [29],

$$\mathcal{L}[c](z) = \frac{c}{z}, \quad (\text{A18})$$

to obtain

$$Z(T, P) = \frac{1}{(\Delta V)\Lambda(T)^N (\beta P)^2} [\Omega(T, P)]^{N-1}. \quad (\text{A19})$$

Here  $\Omega(T, P)$  is defined in Eq. (4).

## APPENDIX B: LOW- $T$ LIMIT

In order to derive properties of the free energy at low temperature approaching the point  $C'$  ( $T=0, P=P_{\text{up}}$ ), we note that in Eq. (7) as  $T \rightarrow 0$ , for small  $P$ , the  $\phi\theta_b$  term dominates, while for large  $P$  the  $\phi^\lambda\theta_a$  dominates. In order to find the limit of  $\Psi(T, P)$  and its derivatives, we note that

$$\frac{\phi^\lambda\theta_a}{\phi\theta_b} = \exp\{\beta[P(b-a) - (1-\lambda)\epsilon]\}. \quad (\text{B1})$$

The value of  $P$  where the  $\phi\theta_b$  term balances the  $\phi^\lambda\theta_a$  term follows equating the argument of the exponential to zero in

Eq. (B1). The result for  $P_{\text{up}}$  is given in Eq. (12). Using Eqs. (12) and (B1), Eq. (7) becomes

$$\Psi(T, P) \sim \phi^\alpha \theta_x \{1 + \exp[-\beta(b-a)|P - P_{\text{up}}|]\}, \quad (\text{B2})$$

where

$$\begin{aligned} \alpha = 1, \quad \theta_x = \theta_b \quad (P < P_{\text{up}}), \\ \alpha = \lambda, \quad \theta_x = \theta_a \quad (P > P_{\text{up}}). \end{aligned} \quad (\text{B3})$$

For  $\partial\Psi(T, P)/\partial P$  we use Eq. (B2) and  $\partial\theta_x/\partial P = -\beta x\theta_x$  to find

$$\frac{\partial\Psi(T, P)}{\partial P} \sim -(\beta x)\Psi(T, P), \quad (\text{B4})$$

where  $x=b$  for  $b < P_{\text{up}}$  and  $x=a$  for  $b > P_{\text{up}}$ . Using Eqs. (B3), (B2), and (B4) in Eq. (9) leads to Eq. (13).

To find the scaling form of  $K_T$  for  $T \rightarrow 0$ , we use the equation for the second derivative of  $\Psi(T, P)$ ,

$$\frac{\partial^2\Psi(T, P)}{\partial P^2} \propto (\beta x)^2 \Psi(T, P). \quad (\text{B5})$$

From Eq. (16), we find  $K_T$  for any  $P \neq P_{\text{up}}$  to behave as

$$K_T \sim (\beta v P^2)^{-1} = (P + \beta x P^2)^{-1} \quad (T \rightarrow 0, P \neq P_{\text{up}}), \quad (\text{B6})$$

which is consistent with Eq. (18).

In order to derive the limiting expressions for the entropy and specific heat, we must differentiate the free energy with respect to  $\beta$ . We start by rewriting Eq. (5) as

$$g(T, P) \equiv \frac{G}{N} = k_B T \ln(\Lambda/\Omega) = k_B T \left( \frac{3}{2} \ln \beta - \ln \Psi(T, P) + \ln P + \text{const} \right). \quad (\text{B7})$$

For  $\Psi(T, P)$  we rewrite Eq. (B2) as

$$\Psi(T, P) \sim E(T, P) \times [1 + w(T, P)], \quad T \rightarrow 0 \quad (\text{B8})$$

with the definitions

$$E(T, P) \equiv \exp[\beta(\epsilon\alpha - Px)], \quad (\text{B9})$$

$$w(T, P) \equiv \exp(-\beta)(b-a)|P - P_{\text{up}}|.$$

Using these definitions, we find

$$\partial \Psi(T, P) / \partial \beta^\alpha (\epsilon\alpha - Px) E [1 + e(1 - T)], \quad (\text{B10})$$

$$\partial^2 \Psi(T, P) / \partial \beta^{2\alpha} (\epsilon\alpha - Px)^2 E [1 + e(1 - T)^2].$$

Using the above equations and Eq. (24), we find

$$C_P = \frac{3}{2} + \beta^2 (\epsilon\alpha - Px)^2 \left( \frac{1 + w(1 - t)^2}{1 + w} - \frac{[1 + w(1 - t)]^2}{(1 + w)^2} \right), \quad (\text{B11})$$

whose leading term is Eq. (28).

- 
- [1] P. G. Debenedetti, *Metastable Liquids* (Princeton University Press, Princeton, 1996).
- [2] O. Mishima and H.E. Stanley, *Nature (London)* **396**, 329 (1998).
- [3] Y. Yoshimura, *Ber. Bunsenges. Phys. Chem.* **95**, 135 (1991), and references therein.
- [4] P.C. Hemmer and G. Stell, *Phys. Rev. Lett.* **24**, 1284 (1970); G. Stell and P.C. Hemmer, *J. Chem. Phys.* **56**, 4274 (1972); J.M. Kincaid, G. Stell, and C.K. Hall, *ibid.* **65**, 2161 (1976); J.M. Kincaid, G. Stell, and E. Goldmark, *ibid.* **65**, 2172 (1976); J.M. Kincaid and G. Stell, *Phys. Lett.* **65A**, 131 (1978); C.K. Hall and G. Stell, *Phys. Rev. A* **7**, 1679 (1973).
- [5] P.G. Debenedetti, V.S. Raghavan, and S.S. Borick, *J. Phys. Chem.* **95**, 4540 (1991); P.G. Debenedetti and M.C. Dantonio, *AIChE J.* **34**, 447 (1988).
- [6] F.H. Stillinger and D.K. Stillinger, *Physica A* **244**, 358 (1997); F.H. Stillinger and T.A. Weber, *J. Chem. Phys.* **68**, 3837 (1978); **74**, 4015 (1981).
- [7] K.K. Mon, N.W. Ashcroft, and G.V. Chester, *Phys. Rev. B* **19**, 5103 (1979); I. Yokoyama and S. Ono, *J. Phys. F* **15**, 1215 (1985); K. Hoshino *et al.*, *ibid.* **17**, 787 (1987).
- [8] T. Head-Gordon and F.H. Stillinger, *J. Chem. Phys.* **98**, 3313 (1993).
- [9] D.A. Young, *J. Chem. Phys.* **58**, 1647 (1973).
- [10] M.R. Sadr-Lahijany, A. Scala, S.V. Buldyrev, and H.E. Stanley, *Phys. Rev. Lett.* **81**, 4895 (1998).
- [11] A detailed description of the results for the 2D simulations that are the subject of [10] is provided in A. Scala, M. R. Sadr-Lahijany, N. Giovambattista, S. V. Buldyrev, and H. E. Stanley (unpublished).
- [12] With these values, the discrete potential has a form similar to the continuous version of the core-softened potential used in 2D [10]. Nevertheless, the behavior we find holds for any range of these parameters, as long as  $0 < a < b < c < 2a$ ,  $\epsilon > 0$ , and  $\lambda < 1$ .
- [13] A. Ben-Naim, *Statistical Thermodynamics for Chemists and Biochemists* (Plenum Press, New York, 1992), pp. 233–238. See, especially, Fig. 4.9, p. 233.
- [14] C. H. Cho, S. Singh, and G. W. Robinson, *Phys. Rev. Lett.* **76**, 1651 (1996), reproduced the density anomaly found by Ben-Naim [13].
- [15] M. Canpolat, F.W. Starr, A. Scala, M.R. Sadr-Lahijany, O. Mishima, S. Havlin, and H.E. Stanley, *Chem. Phys. Lett.* **294**, 9 (1998); (unpublished).
- [16] H. Takahashi, *Proc. Phys. Math. Soc. Jpn.* **24**, 60 (1942); reprinted in *Mathematical Physics in One Dimension*, edited by E. H. Lieb and D. C. Mattis (Academic, New York, 1966) pp. 25–34.
- [17] G.M. Bell and H. Sallouta, *Mol. Phys.* **29**, 1621 (1975).
- [18] F. Sciortino, P.H. Poole, U. Essmann, and H.E. Stanley, *Phys. Rev. E* **55**, 727 (1997).
- [19] S. Sastry, P. Debenedetti, F. Sciortino, and H.E. Stanley, *Phys. Rev. E* **53**, 6144 (1996).
- [20] R.J. Speedy, *J. Phys. Chem.* **86**, 982 (1982).
- [21] P.H. Poole, F. Sciortino, U. Essmann, and H.E. Stanley, *Phys. Rev. E* **48**, 3799 (1993).
- [22] S.T. Harrington, R. Zhang, P.H. Poole, F. Sciortino, and H.E. Stanley, *Phys. Rev. Lett.* **78**, 2409 (1997).
- [23] S. Harrington, P.H. Poole, F. Sciortino, and H.E. Stanley, *J. Chem. Phys.* **107**, 7443 (1997).
- [24] For  $d > 1$ , this can be accompanied by an increase of the diffusion constant  $D$ . This anomalous increase in diffusion is observed both in simulations and in water [10,26].
- [25] A  $T_{\text{MD}}$  line meeting a critical point has been observed in simulations of confined water [M. Meyer and H.E. Stanley, *J. Phys. Chem.* **103**, 9728 (1999)].
- [26] F.W. Starr, S. Harrington, F. Sciortino, and H.E. Stanley, *Phys. Rev. Lett.* **82**, 3629 (1999); F. W. Starr, F. Sciortino, and H. E. Stanley, *Phys. Rev. E* **60**, 6757 (1999).
- [27] P. M. Chaikin and T. C. Lubensky, *Principles of Condensed Matter Physics* (Cambridge University Press, Cambridge, 1995).
- [28] P.H. Poole, F. Sciortino, U. Essmann, and H.E. Stanley, *Nature (London)* **360**, 324 (1992); *Phys. Rev. E* **48**, 4605 (1993); O. Mishima and H.E. Stanley, *ibid.* **392**, 164 (1998).
- [29] I. S. Gradshteyn and I. M. Ryzhik, *Table of Integrals, Series, and Products* (Academic Press, London, 1980).